

Theory of quantum radiation observed as sonoluminescence

Claudia Eberlein[§]

Department of Physics

University of Illinois at Urbana-Champaign

Urbana, IL 61801-3080

U.S.A.

(Submitted June 7, 1995)

Abstract

Sonoluminescence is explained in terms of quantum radiation by moving interfaces between media of different polarizability. In a stationary dielectric the zero-point fluctuations of the electromagnetic field excite virtual two-photon states which become real under perturbation due to motion of the dielectric. The sonoluminescent bubble is modelled as an optically empty cavity in a homogeneous dielectric. The problem of the photon emission by a cavity of time-dependent radius is handled in a Hamiltonian formalism which is dealt with perturbatively up to first order in the velocity of the bubble surface over the speed of light. A parameter-dependence of the zero-order Hamiltonian in addition to the first-order perturbation calls for a new perturbative method combining standard perturbation theory with an adiabatic approximation. In this way the transition amplitude from the vacuum into a two-photon state is obtained, and expressions for the single-photon spectrum and the total energy radiated during one flash are given both in full and in the short-wavelengths approximation when the bubble is larger than the wavelengths of the emitted light. A model profile is assumed for the time-dependence of the bubble during the collapse, and in this model the radiated energy and the spectrum are calculated numerically and in the short-wavelengths limit also analytically. It is shown analytically that the spectral density has the same frequency-dependence as black-body radiation; this is purely an effect of correlated quantum fluctuations at zero temperature. The present theory clarifies a number of hitherto unsolved problems and suggests explanations for several more. Possible experiments that discriminate this from other theories of sonoluminescence are proposed.

PACS numbers: 03.70.+k, 11.10.-z, 42.50.Lc, 78.60.Mq

[§]e-mail to: claudia@cromwell.physics.uiuc.edu

1 INTRODUCTION

1.1 State of the art

Sonoluminescence is the phenomenon of light emission by sound-driven gas bubbles in fluids, ordinarily air bubbles in water. Sound makes bubbles collapse or expand, and a rapid flash of light is observed after each collapse. This phenomenon has been known for 60 years [1], but came under systematic investigation only recently when experimentalists succeeded in trapping bubbles and maintaining sonoluminescence as a stable process over hours or even days [2, 3].

During stable sonoluminescence [2, 3] a bubble is trapped at the pressure antinode of a standing sound wave, which typically has a frequency of about 25 kHz. With an astonishing clocklike precision the bubble sends off one sharp flash of light per acoustic cycle. Less than 10 ps is commonly given as a conservative estimate of the pulse length. The observed jitter has been found to be extremely small and to show curious phase properties whose origin could so far not be identified [4]. The spectral density of the light emitted drops with wavelength and resembles the tail of a black-body spectrum of several tens of thousand Kelvin [5].

Whereas the dynamics of the bubble motion has been successfully explained and a theoretical model by Löfstedt, Barber, and Putterman [6] based on rather involved hydrodynamic calculations reproduces the experimentally measured time-dependence of the bubble radius [7] remarkably well, the process of the light emission has so far defied any theoretical elucidation. That is why the present paper focuses on the radiation process, making use of the knowledge about the hydrodynamics of the bubble motion as input.

There have been several attempts of explaining the light seen in sonoluminescence. The apparent similarity of the spectrum to a thermal spectrum has led to the hypothesis that the light might come from a process of black-body radiation or bremsstrahlung [5, 8]. Along this line it has been argued that the gas in the collapsing bubble is compressed so strongly that a plasma is formed which then radiates. However, one can quickly convince oneself that neither black-body radiation nor bremsstrahlung can possibly account for the radiation observed in sonoluminescence. Either of them would lead to a continuous spectrum whose major part would lie below the absorption edge of water at 180nm and would therefore be absorbed by it. Estimating from the corresponding visible part of the spectrum the amount of energy that would be absorbed, one obtains such a large number that one would expect to see rather obvious macroscopic consequences of the absorption [9], as for instance dissociation of the water molecules, formation of radicals etc., which have not been observed. Moreover, black-body radiation is an equilibrium phenomenon and involves several atomic transitions; it could very unlikely explain pulse lengths of less than 10ps. Neither is any explanation involving bremsstrahlung satisfactory, because it would entail the presence of free electrons and rather slow recombination radiation.

Rather more convincing is Suslick's theory [10] which explains the sonoluminescence spectra on the basis of pressure-broadened rotational and vibrational lines in diatomic emission spectra. For silicone-oil sonoluminescence one finds an excellent agreement of synthetic and observed spectra by considering emission from excited-state C_2 [10]. For water, however, any attempts to model the spectrum on the basis of this theory have so far been unsuccessful,

although the well-known 310nm system of OH is thought to be largely responsible for the broad peak around this wavelength in the observed spectrum [9, 11].

The most recent speculation on the nature of sonoluminescence radiation is a theory of collision-induced emission [12], which, however, in its present version contains still too many indeterminate points and adjustable parameters to permit a judgement on its tenability.

1.2 Quantum vacuum radiation as a candidate

This article pursues a line of thought loosely inspired by Schwinger [13] who suggested that sonoluminescence could be some kind of dynamic Casimir effect, which the present writer agrees with in so far as the light emission observed in sonoluminescence has, just like the Casimir effect, its origin in the interaction of the vacuum fluctuations of the quantized electromagnetic field with a dielectric medium. Sonoluminescence is, however, much more closely related to the Unruh effect.

Let first the Casimir effect [14, 15] be recalled: two parallel conducting or dielectric plates in vacuum feel an attractive force which arises from the boundary conditions the plates impose on the vacuum electromagnetic field. In a more intuitive picture one can understand the Casimir effect in terms of van-der-Waals forces; the electromagnetic zero-point fluctuations induce local fluctuating dipoles in each of the plates and because of the spatial correlations of the fluctuations the interaction of these dipoles leads to a net attractive force.

The Unruh effect [16, 17] is a dynamic generalization of the Casimir effect and predicts radiation by non-inertially moving mirrors. This phenomenon is not exclusive to perfect mirrors, i.e. perfect conductors; quantum radiation by moving dielectrics has also been investigated [18], and moreover some of the pathological points of the perfect-reflector theories can be circumvented in the more physical case of dielectrics. Again, the intuitive picture of the process is that the zero-point electromagnetic field excites fluctuating dipoles in the (perfect or imperfect) mirror and these dipoles are the source of radiation when the mirror moves non-uniformly.

A more rigorous way of understanding why a moving mirror that interacts with the vacuum fluctuations of the quantized photon field emits radiation, is to start by considering a nominally stationary mirror, with the intention of eventually applying the fluctuation-dissipation theorem. The radiation pressure on the mirror is given by the vacuum expectation value of the force operator \mathcal{F} , which is obtained from the stress-energy-momentum tensor of the electromagnetic field subjected to appropriate boundary conditions on the surface of the mirror. The net force on a single stationary mirror in vacuum is of course zero by virtue of translation invariance,

$$F = \langle 0 | \mathcal{F} | 0 \rangle = 0 .$$

However, the mean-square deviation of this force does not vanish, since the force operator \mathcal{F} does not commute with the Hamiltonian. In other words, the mirror is exposed to radiation-pressure fluctuations, whose mean-square deviation is given by

$$\Delta F^2 = \langle 0 | \mathcal{F}^2 | 0 \rangle - \langle 0 | \mathcal{F} | 0 \rangle^2 .$$

Knowing that the force operator \mathcal{F} is (just like the Hamiltonian) a functional that is quadratic in the field operators, i.e. quadratic in the photon annihilation and creation operators, one

can use the decomposition of the identity into projection operators onto a complete set of photon eigenstates, of which then only two-photon states survive, and rewrite [19]:

$$\Delta F^2 = \frac{1}{2} \int dk \int dk' |\langle 0 | \mathcal{F} | k, k' \rangle|^2. \quad (1.1)$$

This means that virtual two-photon states are perpetually excited by the mirror in the vacuum, in accordance with the fluctuating radiation pressure. Yet the fluctuating forces on the left and right sides of the mirror are balanced against each other, so that no mean radiation pressure acts on the mirror. By virtue of Lorentz invariance, the same is true for a mirror that moves with constant velocity.

However, when the mirror moves non-inertially, the radiation-pressure fluctuations on opposite sites of the mirror are out of balance and the mirror experiences a non-vanishing frictional force. The virtual two-photon states turn into real states, and the loss of momentum by the radiation of the photon pairs provides the physical mechanism for the friction felt by the mirror. The fluctuation-dissipation theorem puts this into formulae and interrelates the power spectrum of the fluctuations on the stationary mirror and the dissipative part of the response function that connects the force on the moving mirror to its velocity [20].

It is a well-established fact that radiation by moving mirrors shows thermal properties although one is dealing with *zero*-temperature quantum field theory. The original statement of the Unruh effect [16, 17] is that a mirror moving with constant proper acceleration a in vacuum appears to be radiating particles as if it were a black body at a temperature $T_{\text{Unruh}} = \hbar a / (2\pi k_B c)$. The reason for this behaviour is that the photons are radiated in correlated pairs, in the language of quantum optics — they form a two-mode squeezed state, and the observation of the single-photon spectrum involves a tracing over the other photon of the pair which is well-known to entail thermal properties of the state [21]. Formally this connection is established by representing the two-mode state in a dual Hilbert space and making contact with the theory of thermofield dynamics [22].

As to an experimental verification of the Unruh effect, the record is empty. Understandably so, because the Unruh temperature is tiny for commonly achievable accelerations. The only viable suggestion for an experiment has come from Yablonovitch [23], who thought that the sudden ionization of a gas or a semiconductor crystal might produce an accelerating discontinuity in the refractive index fast enough to radiate a measurable amount of photons.

From all of the above, quantum vacuum radiation seems to be a good candidate for explaining the radiation process in sonoluminescence. The surface of the bubble is the moving interface of discontinuous polarizability, i.e. the moving mirror. In the visible range water has a refractive index of 1.3, and the gas inside the bubble has a refractive index of practically 1 even when strongly compressed. Although the discontinuity of 0.3 in the refractive index is not huge, it is large enough to radiate an appreciable number of photons if the motion is sufficiently fast. In fact, the discontinuity in the refractive index will enter the final results for the radiated spectrum merely as a prefactor, and hence only its order of magnitude is important.

Of much greater significance is the highly non-linear dynamics of the bubble motion. At the point when the bubble collapses and starts re-expanding, the velocity of the interface changes its sign. As known from experiments [7] as well as from model calculations of the bubble dynamics [6, 8] this turn-around is extremely fast, which means that tremendous

accelerations and higher moments of the motion are involved. The present theory predicts a burst of photons as a consequence.

As it will be shown in more detail in the course of this article, the theory of quantum vacuum radiation resolves several to date unexplained issues.

The fact that the photons are radiated in correlated pairs leads to thermal properties of the one-photon spectrum, unrelated to the temperature in the bubble which is presumably far too small to cause any major effect.

In accordance with a weakly frequency-dependent refractive index the radiation spectrum shows features at the resonance frequencies of the dipolar molecules in the medium. As water molecules are highly polarizable, this is to be expected a discernible effect; it explains the relation of the peak around 310nm in the spectrum to the well-known OH line.

Barely any photons are created below the absorption edge of water, as the polarizability is far too small in this region. Therefore, few photons are absorbed and no macroscopically noticeable changes of the water are to be expected.

The pulse length predicted by the theory of quantum vacuum radiation is of the order of the time it takes for the zero-point fluctuations to correlate around the bubble. With bubble sizes of around $1\mu\text{m}$ or less, the time light takes to cross the bubble is in the femtosecond range. Otherwise the time-scale is of course influenced by the dynamics of the motion of the bubble interface at and just after the collapse.

1.3 Outline and overview

The theory of quantum vacuum radiation by a gas bubble in water will be expounded in the following sections. Water will be understood as a non-absorbing dielectric describable by a constant refractive index. This is a good approximation in the spectral region of interest where water is only weakly dispersive. By virtue of adiabaticity the refractive index n can be replaced by $n(\omega)$ in the end result for the radiated spectrum. The gas inside the bubble is optically so thin, even at the collapse of the bubble, that its refractive index will be assumed to be 1 throughout the calculation.

The bubble will be considered as externally driven, i.e. the radius of the bubble as a prescribed function of time; the hydrodynamics of the bubble motion is not the concern of this paper. However, the back-reaction of the radiation process on the motion of the bubble will be specified.

Hence the problem is reduced to a model of a spherical cavity of radius $R(t)$ in a homogeneous non-dispersive dielectric described by a constant refractive index n . The radiated spectral density will be obtained as a functional of $R(t)$.

The next section deals with the quantization of the photon field in the presence of a stationary spherical bubble in a homogeneous dielectric. In section III the Schrödinger equation for the photon state-vector is written down, and the vacuum-to-two-photon transition-amplitude is calculated by a method of time-dependent perturbation theory that accommodates both an adiabatic time-dependence of the Hamiltonian and a perturbative addition to the zero-order Hamiltonian [24]. Section IV states and examines the results for the radiated energy and the spectral density. The appearance of a thermal-like spectrum is demonstrated and numerical results are presented. Finally, section V gives a summary and a critical reflection on the theory of quantum vacuum radiation by sonoluminescent bubbles. Strengths

and weaknesses of the theory are scrutinized, and open questions are voiced.

Readers not interested in the technicalities of the theory are encouraged to look over section IV for an aggregate of the essential results and to read section V for a guided summary and interpretation of all results.

Several appendices contribute technical details necessary for the clarity of the presentation. Appendix A calculates the Hamiltonian for a uniformly moving dielectric in preparation for section III. Appendix B gives the mode-expansion for the Helmholtz equation in spherical coordinates, which is essential throughout the paper. The force on a stationary dielectric is determined in appendix C.

CGS units are used everywhere in the paper; \hbar and c are set equal to 1 unless explicitly indicated. All special functions are defined as in refs. [25, 26].

2 QUANTIZATION OF THE PHOTON FIELD

The Hamiltonian for the electromagnetic field in the presence of a medium with dielectric function $\varepsilon(\mathbf{r})$ reads

$$H_0 = \frac{1}{2} \int d^3\mathbf{r} \left(\frac{\mathbf{D}^2}{\varepsilon} + \mathbf{B}^2 \right) . \quad (2.1)$$

A bubble of radius R is described by

$$\varepsilon(r; R) = 1 + (n^2 - 1) \theta(r - R) , \quad (2.2)$$

where θ is the Heaviside step function. This is to say that the dielectric constant equals 1 in the interior of the bubble and n^2 in the surrounding medium. The Maxwell equations imply continuity conditions for the fields across the boundary; these are:

$$\begin{aligned} \mathbf{D}_\perp \text{ and } \frac{\mathbf{D}_\parallel}{\varepsilon} \text{ continuous ,} \\ \mathbf{B} \text{ continuous ,} \end{aligned} \quad (2.3)$$

or in spherical coordinates

$$\begin{aligned} \mathbf{D}_r^{\text{inside}} = \mathbf{D}_r^{\text{outside}} , \quad \mathbf{D}_\theta^{\text{inside}} = \frac{\mathbf{D}_\theta^{\text{outside}}}{n^2} , \quad \mathbf{D}_\phi^{\text{inside}} = \frac{\mathbf{D}_\phi^{\text{outside}}}{n^2} , \\ \mathbf{B}_r^{\text{inside}} = \mathbf{B}_r^{\text{outside}} , \quad \mathbf{B}_\theta^{\text{inside}} = \mathbf{B}_\theta^{\text{outside}} , \quad \mathbf{B}_\phi^{\text{inside}} = \mathbf{B}_\phi^{\text{outside}} . \end{aligned} \quad (2.4)$$

The Hamiltonian (2.1) depends parametrically on the bubble radius R via the dielectric function $\varepsilon(r; R)$. Although a problem with a varying bubble size is aspired to be solved, for the purpose of quantizing the photon field the radius of the bubble will be kept constant. In order to quantize the system for a time-dependent radius $R(t)$ one would need to know the eigenfunctions of the time-dependent Hamiltonian (A6); but knowing them would amount to the exact solution of the whole problem which is of course unachievable. As the calculation to follow in the next section will employ perturbation theory to first order in the velocity of the bubble surface $\beta = \dot{R}(t)$ over the speed of light in vacuum, a quantization for constant R is fully sufficient.

The field is quantized by ascribing operator nature to the field variables and imposing canonical commutation relations for the vector field \mathbf{A} and its conjugate momentum $\mathbf{\Pi} = -\mathbf{D}$. These are most easily implemented by expanding the field operators in terms of photon annihilation and creation operators, $a_{\mathbf{k}}^s$ and $a_{\mathbf{k}}^{s\dagger}$ respectively for a mode of momentum \mathbf{k} and polarization s , and demanding that the latter fulfil the standard commutation relations

$$\begin{aligned} [a_{\mathbf{k}}^s, a_{\mathbf{k}'}^{s'\dagger}] &= \delta(\mathbf{k} - \mathbf{k}') \delta_{ss'} , \\ [a_{\mathbf{k}}^s, a_{\mathbf{k}'}^{s'}] &= 0 . \end{aligned} \quad (2.5)$$

At the same time the normal-mode expansions should be chosen such as to diagonalize the Hamiltonian (2.1) to the Hamiltonian of a photon field

$$H_0 = \sum_s \int d^3\mathbf{k} \omega \left[a_{\mathbf{k}}^{s\dagger} a_{\mathbf{k}}^s + \frac{1}{2} \right] , \quad \omega = |\mathbf{k}| . \quad (2.6)$$

All this is achieved by the following expansion of the electric displacement \mathbf{D} and the magnetic field \mathbf{B} :

$$\begin{aligned} \mathbf{D}_{\text{TE}} &= \varepsilon \int d^3\mathbf{k} \frac{i\omega}{\sqrt{\omega}} \left[a_{\mathbf{k}}^{\text{TE}} \mathbf{A}_{(1)}^{\text{TE}} - \text{H C} \right] , \\ \mathbf{B}_{\text{TE}} &= \sqrt{\varepsilon} \int d^3\mathbf{k} \frac{\omega}{\sqrt{\omega}} \left[a_{\mathbf{k}}^{\text{TE}} \mathbf{A}_{(2)}^{\text{TE}} + \text{H C} \right] , \\ \mathbf{D}_{\text{TM}} &= \varepsilon \int d^3\mathbf{k} \frac{i\omega}{\sqrt{\omega}} \left[a_{\mathbf{k}}^{\text{TM}} \mathbf{A}_{(2)}^{\text{TM}} - \text{H C} \right] , \\ \mathbf{B}_{\text{TM}} &= \sqrt{\varepsilon} \int d^3\mathbf{k} \frac{\omega}{\sqrt{\omega}} \left[a_{\mathbf{k}}^{\text{TM}} \mathbf{A}_{(1)}^{\text{TM}} + \text{H C} \right] . \end{aligned} \quad (2.7)$$

The mode functions $\mathbf{A}_{(1,2)}$ are two linearly independent solutions of the Helmholtz equation. They satisfy the Coulomb gauge condition $\nabla \cdot \mathbf{A}_{(1,2)} = 0$. The fields have been decomposed into their two transverse polarizations, chosen in spherical coordinates as the transverse electric (TE), for which the radial component of the displacement \mathbf{D} vanishes, and the transverse magnetic (TM), for which the radial component of the magnetic field \mathbf{B} vanishes. The mode functions $\mathbf{A}_{(1,2)}$ and their properties are spelled out in appendix B.

As mentioned above the quantization procedure is performed at an arbitrary but constant bubble radius R . This implies that although the Hilbert space of the quantized system stays always the same, the set of base vectors spanning it changes with R . A unitary transformation from the base at radius R to the one at radius R' exists in principle, but is hard if not impossible to find explicitly. So the bubble radius R serves as a parameter in traversing a continuous sequence of bases, and in a strict notation the photon annihilation and creation operators and the photon eigenstates should be supplemented by a label R . The vacuum or ground state of the field is defined by

$$a_{\mathbf{k}}^s(R) | 0; R \rangle = 0 , \quad \langle 0; R | 0; R \rangle = 1 ;$$

single-photon states are written as

$$| k_s; R \rangle = a_{\mathbf{k}}^{s\dagger}(R) | 0; R \rangle , \quad \langle k_s; R | k_{s'}^{\prime}; R \rangle = \delta(k - k') \delta_{ss'} ;$$

two-photon states are denoted by

$$\begin{aligned} |k_s, k'_s; R\rangle &= a_k^{s\dagger}(R) a_{k'}^{s'\dagger}(R) |0; R\rangle, \\ \langle k_s, k'_s; R | l_p, l'_p; R\rangle &= \delta(k - l) \delta_{sp} \delta(k' - l') \delta_{s'p'} + \delta(k - l') \delta_{sp'} \delta(k' - l) \delta_{s'p}; \end{aligned}$$

and so on for all higher photon number states.

3 TWO-PHOTON EMISSION IN FIRST-ORDER PERTURBATION THEORY

The evolution of the state vector $|\psi\rangle$ of the photon field is governed by the Schrödinger equation

$$i \frac{d}{dt} |\psi\rangle = [H_0(R) + \Delta H(R, \beta)] |\psi\rangle \quad (3.1)$$

where, according to the Hamiltonian (A6) derived in appendix A,

$$H_0 = \frac{1}{2} \int d^3\mathbf{r} \left(\frac{\mathbf{D}^2}{\varepsilon} + \mathbf{B}^2 \right), \quad (3.2a)$$

$$\Delta H = \beta \int d^3\mathbf{r} \frac{\varepsilon - 1}{\varepsilon} (\mathbf{D} \wedge \mathbf{B})_r, \quad (3.2b)$$

and $\beta \equiv \dot{R}$ is the velocity of the bubble surface.

For the present purposes antisymmetrization of the operator product in ΔH can be dispensed with. What will be extracted from the mode expansion of $(\mathbf{D} \wedge \mathbf{B})_r$ are products of two photon creation operators $a_k^\dagger a_{k'}^\dagger$ which induce two-photon transitions from the vacuum. Since, however, creation operators commute mutually, operator ordering is inessential.

To describe the sonoluminescence process by the Hamiltonian (3.2) means to ignore variations of the refractive index due to the periodic compression of the water in the vicinity of the bubble. This is a crude but innocuous approximation as long as the energies of the phonons excited in the water stay below those of the emitted photons.

Initially the photon field is in its vacuum state while the bubble is at rest and has some radius R . As discussed at the end of the preceding section, the photon eigenstates depend parametrically on the radius R of the bubble. Hence the initial condition for the state vector $|\psi\rangle$ reads

$$|\psi(t_0)\rangle = |0; R(t_0)\rangle. \quad (3.3)$$

The integration of the Schrödinger equation (3.1) poses a non-trivial problem since standard methods of perturbation theory cannot be applied. The Hamiltonian ΔH (3.2b) cannot be treated as an ordinary perturbation because ΔH as well as H_0 depend on the parameter R . The established way of dealing with slowly parameter-dependent Hamiltonians is the adiabatic approximation [27]. However, the standard adiabatic approximation requires the knowledge of the complete set of eigenfunctions of the Hamiltonian for any allowed value of the parameter. In the present case only the eigenfunctions of part of the Hamiltonian, namely those of H_0 , are known. Hence what is required is a judicious combination of standard perturbation theory and the standard adiabatic approximation; needed is a theory that is

capable of dealing both with a perturbative interaction Hamiltonian and with a Hamiltonian depending on a slowly varying parameter.

Following the adiabatic theory by Pauli [27], one starts with the eigenvalue equation for the unperturbed Hamiltonian H_0 , solved for all possible values of the parameter R

$$H_0(R) |n(R)\rangle = E_n(R) |n(R)\rangle, \quad (3.4)$$

where $E_n(R)$ is the n th eigenvalue and $|n(R)\rangle$ the corresponding eigenvector. Here n is just a label; the eigenvalue spectrum need not be discrete. In general the levels can be multiply degenerate, so that $|n(R)\rangle$ in fact stands for a whole subspace of orthonormal eigenvectors to the same eigenvalue $E_n(R)$. Where degeneracy matters it will be explicitly indicated by states $|n'(R)\rangle$ also belonging to $E_n(R)$.

Differentiating (3.4) with respect to R and calculating the overlap with a state $\langle m(R)|$ one obtains

$$\langle m|\frac{\partial H_0}{\partial R}|n\rangle + E_m\langle m|\frac{\partial}{\partial R}|n\rangle = \frac{\partial E_n}{\partial R}\langle m|n\rangle + E_n\langle m|\frac{\partial}{\partial R}|n\rangle.$$

Thus, provided no level-crossing occurs, ie if for $m \neq n$ is $E_m(R) - E_n(R)$ is different from zero for all possible R , as it will be the case in the present application, one has

$$\langle m|\frac{\partial}{\partial R}|n\rangle = \frac{1}{E_n - E_m}\langle m|\frac{\partial H_0}{\partial R}|n\rangle \quad \text{for } m \neq n. \quad (3.5)$$

Seeking a solution of the Schrödinger equation (3.1), one expands the wave-vector $|\psi(t)\rangle$ into the eigenvectors of the instantaneous $H_0(R(t))$

$$|\psi(t)\rangle = \sum_n |n(R(t))\rangle \langle n(R(t))|\psi(t)\rangle. \quad (3.6)$$

Then the Schrödinger equation (3.1) becomes

$$\sum_n \left[i \left(\frac{\partial}{\partial R} |n\rangle \right) \frac{\partial R}{\partial t} \langle n|\psi\rangle + i |n\rangle \left(\frac{\partial}{\partial t} \langle n|\psi\rangle \right) \right] = \sum_n [E_n |n\rangle \langle n|\psi\rangle + \Delta H |n\rangle \langle n|\psi\rangle],$$

which by taking the scalar product with an eigenstate $\langle m|$ is turned into

$$\sum_n i\beta \langle n|\psi\rangle \langle m|\frac{\partial}{\partial R}|n\rangle + i \frac{\partial}{\partial t} \langle m|\psi\rangle = E_m \langle m|\psi\rangle + \sum_n \langle m|\Delta H|n\rangle \langle n|\psi\rangle.$$

From here, application of the relation (3.5) yields

$$\begin{aligned} i \frac{\partial}{\partial t} \langle m|\psi\rangle - E_m \langle m|\psi\rangle + i\beta \sum_{m'(E_{m'}=E_m)} \langle m'|\psi\rangle \langle m|\frac{\partial}{\partial R}|m'\rangle \\ = -i\beta \sum_{n(n \neq m)}' \frac{\langle n|\psi\rangle}{E_n - E_m} \langle m|\frac{\partial H_0}{\partial R}|n\rangle + \sum_n \langle m|\Delta H|n\rangle \langle n|\psi\rangle, \end{aligned}$$

where the sum over m' takes states degenerate with m into account. Since eventually the transition probability $|\langle m|\psi\rangle|^2$ and not the transition amplitude $\langle m|\psi\rangle$ will be of physical

interest, one can gauge away the second term on the left-hand side of the above equation by defining

$$\langle m|\psi\rangle = c_m \exp \left[-i \int_{t_0}^t d\tau E_m(\tau) \right] ; \quad (3.7)$$

one finds

$$\begin{aligned} \frac{\partial c_m}{\partial t} + \beta \sum_{m' (E_{m'}=E_m)} c_{m'} \langle m|\frac{\partial}{\partial R}|m'\rangle \\ = \beta \sum_{n (n \neq m)}' \frac{c_n}{E_n - E_m} \langle m|\frac{\partial H_0}{\partial R}|n\rangle \exp \left[i \int_{t_0}^t d\tau (E_m - E_n) \right] \\ - i \sum_n' c_n \langle m|\Delta H|n\rangle \exp \left[i \int_{t_0}^t d\tau (E_m - E_n) \right] , \end{aligned} \quad (3.8)$$

which is the key formula for the present approximation method. If it were not for the term containing ΔH , this expression would lead to merely the standard adiabatic approximation (cf. for instance ref. [28]). It should be noted that both terms on the right-hand side of (3.8) are of the same order, namely β^1 ; the matrix element of $\partial H_0/\partial R$ is multiplied by β , and ΔH is itself of order β .

The initial condition (3.3) for the wave function $|\psi\rangle$ translates into the following initial conditions for the coefficients $c_m(t)$ defined by (3.7)

$$c_0(t_0) = 1 , \quad c_{m \neq 0}(t_0) = 0 . \quad (3.9)$$

As soon as the bubble starts moving, ie the interface velocity $\beta(t > t_0)$ becomes different from zero, the rate of change of the c_m is non-zero, as described by eq (3.8). For times $t > t_0$ one has $c_0(t) \approx 1$ and $c_{m \neq 0}(t) = O(\beta)$ or higher. Hence, working only to first order in β , one has to retain only the vacuum state in the summation over n on the right-hand side of eq (3.8).

Handling the time-dependence of the energy eigenvalues E_n requires special care. For a cavity, like the bubble in the present problem, one has two limiting cases. The first is that the cavity walls are very poor reflectors; then it is convenient to label the cavity modes by wavenumber or energy as these are adiabatically conserved. However, if the cavity has a very high Q value, i.e. is close to perfectly reflecting, the number of nodes of the eigenfunction will be the adiabatically conserved quantity and not the wavenumber. The probability of reflection from an interface of a medium of refractive index n with the vacuum is given by $(n-1)^2/(n+1)^2$. For an air-water interface in the visible spectrum where $n = 1.3$ this leads to a reflection probability of less than 2%. Hence the bubble is a poor-quality cavity and the energy eigenvalues are adiabatically conserved. This justifies the use of wavenumbers for the labelling of eigenstates.

Since H_0 , and hence $\partial H_0/\partial R$, and ΔH are quadratic in the fields, the only transitions they can induce from the initial vacuum state lead to two-photon states, whence to first order in β [29] the system of differential equations (3.8) for the coefficients c_m reduces to

$$\frac{\partial c_0}{\partial t} + \beta \langle 0; R|\frac{\partial}{\partial R}|0; R\rangle = -i \langle 0; R|\Delta H|0; R\rangle , \quad (3.10a)$$

$$\frac{\partial c_{kk'}}{\partial t} = \beta \frac{1}{\omega + \omega'} \langle k, k'; R|\frac{\partial H_0}{\partial R}|0; R\rangle e^{i(\omega + \omega')(t-t_0)} - i \langle k, k'; R|\Delta H|0; R\rangle e^{i(\omega + \omega')(t-t_0)} . \quad (3.10b)$$

The first equation is of no special interest, but the second equation will readily provide the solution of the problem posed — the perturbative description of the photon creation by the moving bubble surface. According to (3.7) the transition amplitude from the vacuum into a two-photon state is given by

$$\langle k, k'; R | \psi \rangle = c_{kk'}(t) e^{-i(\omega+\omega')(t-t_0)}, \quad (3.11)$$

and the initial vacuum evolves into the state

$$|\psi\rangle = |0; R\rangle + \frac{1}{2} \int_{-\infty}^{\infty} dk \int_{-\infty}^{\infty} dk' c_{kk'}(t) e^{-i(\omega+\omega')(t-t_0)} |k, k'; R\rangle. \quad (3.12)$$

The factor 1/2 takes care of the identical photon states $|k, k'; R\rangle = |k', k; R\rangle$, not to be double counted.

It remains to evaluate the two matrix elements in eq (3.10b). With H_0 as in (3.2a) one finds for the first

$$\langle k, k'; R | \frac{\partial H_0}{\partial R} | 0; R \rangle = \frac{1}{2} \left(1 - \frac{1}{n^2} \right) R^2 \oint d\Omega \langle k, k'; R | D_r^2 + n^2 \mathbf{E}_{\parallel}^2 | 0; R \rangle, \quad (3.13)$$

in the obvious notation $\mathbf{E}_{\parallel} = (E_{\theta}, E_{\phi})$. Deriving this, one should bear in mind that H_0 depends on R both through $\varepsilon(R)$ and through the discontinuity of $\mathbf{D}_{\parallel} = (D_{\theta}, D_{\phi})$.

With ΔH as in (3.2b) the second matrix element in (3.10b) reads

$$\langle k, k'; R | \Delta H | 0; R \rangle = \beta \left(1 - \frac{1}{n^2} \right) \int_{r \geq R} d^3 \mathbf{r} \langle k, k'; R | (\mathbf{D} \wedge \mathbf{B})_r | 0; R \rangle. \quad (3.14)$$

As photon states are eigenstates of H_0 , one can write

$$\begin{aligned} i(\omega + \omega') \langle k, k'; R | (\mathbf{D} \wedge \mathbf{B})_r | 0; R \rangle &= \langle k, k'; R | i [H_0, (\mathbf{D} \wedge \mathbf{B})_r] | 0; R \rangle \\ &= \langle k, k'; R | \frac{\partial}{\partial t} (\mathbf{D} \wedge \mathbf{B})_r | 0; R \rangle. \end{aligned} \quad (3.15)$$

to first order in β . In further manipulating this expression, one can make use of the classical energy-momentum conservation law in a bulk dielectric

$$\frac{\partial}{\partial t} (\mathbf{D} \wedge \mathbf{B})_i + \nabla_j T^{ij} = 0, \quad (3.16)$$

where the stress-tensor in the medium is given by

$$T^{ij} = -\frac{D_i D_j}{\varepsilon} - B_i B_j + \frac{1}{2} \delta_{ij} \left(\frac{\mathbf{D}^2}{\varepsilon} + \mathbf{B}^2 \right). \quad (3.17)$$

Since the photon field is a non-self-interacting field in Minkowski space, there is no doubt that this conservation law is valid also quantally. Using this and the above relation (3.15), one can rewrite (3.14)

$$\langle k, k'; R | \Delta H | 0; R \rangle = i \frac{\beta}{\omega + \omega'} \left(1 - \frac{1}{n^2} \right) \int_{r \geq R} d^3 \mathbf{r} \langle k, k'; R | \nabla_j T^{rj} | 0; R \rangle.$$

Applying Gauss' theorem leads to

$$\begin{aligned} \langle k, k'; R | \Delta H | 0; R \rangle &= -i \frac{\beta R^2}{\omega + \omega'} \left(1 - \frac{1}{n^2}\right) \oint d\Omega \langle k, k'; R | T^{rr} | 0; R \rangle \\ &= -i \frac{\beta R^2}{\omega + \omega'} \left(1 - \frac{1}{n^2}\right) \oint d\Omega \langle k, k'; R | \frac{1}{2} \left(n^2 \mathbf{E}_{\parallel}^2 - \frac{D_r^2}{n^2} + \mathbf{B}_{\parallel}^2 - B_r^2 \right) | 0; R \rangle . \end{aligned} \quad (3.18)$$

Inserting (3.13) and (3.18) into the expression (3.10b) one finds for the time-derivative of the transition amplitude between the vacuum and a two-photon state $|k, k'\rangle$

$$\frac{\partial c_{kk'}}{\partial t} = \left(1 - \frac{1}{n^2}\right) \frac{\beta R^2}{2} \frac{e^{i(\omega+\omega')(t-t_0)}}{\omega + \omega'} \oint d\Omega \langle k, k'; R | \left(1 + \frac{1}{n^2}\right) D_r^2 - \mathbf{B}_{\parallel}^2 + B_r^2 | 0; R \rangle .$$

Comparison with the force operator \mathcal{F}_r given by eq. (C5) uncovers the relation of the photon creation to the pressure on the bubble; $\partial c_{kk'}/\partial t$ can be re-expressed as

$$\frac{\partial c_{kk'}}{\partial t} = -\frac{\beta}{\omega + \omega'} e^{i(\omega+\omega')(t-t_0)} \langle k, k'; R | \mathcal{F}_r | 0; R \rangle . \quad (3.19)$$

This is a truly remarkable result as it exposes the fluctuations of the radiation pressure as the origin of the photon-pair creation. As described by eq. (1.1) for the mean-square deviation of the force, the fluctuations on a stationary mirror are tied in with the excitation of virtual two-photon states. The (non-uniform) motion of a mirror or a dielectric interface makes these virtual states become real, which has been explained in the two paragraphs following eq. (1.1) and is shown manifestly by eq. (3.19). The fluctuation-dissipation theorem underlies this connection; it however predicts only the dissipative force acting on the moving interface and not the photon-creation amplitude. Hence, the fluctuation-dissipation theorem cannot supersede the above derivation, but is nevertheless a useful check on it [20].

The integration of eq. (3.19) is complicated by the fact that the force matrix-element depends parametrically on R and therefore on time. Formally, the transition amplitude reads

$$c_{kk'}(t) = -\frac{1}{\omega + \omega'} \int_{t_0}^t d\tau \beta(\tau) e^{i(\omega+\omega')(\tau-t_0)} \langle k, k'; R(\tau) | \mathcal{F}_r | 0; R(\tau) \rangle . \quad (3.20)$$

The matrix elements of the force operator, which is given by (C5), are calculated by expanding the \mathbf{D} and \mathbf{B} fields into normal modes as detailed in section 2 and appendix B. An unsophisticated calculation yields

$$\begin{aligned} \langle k_{\text{TE}}, k'_{\text{TE}}; R | \mathcal{F}_r | 0; R(\tau) \rangle &= \frac{n}{2\pi} \left(1 - \frac{1}{n^2}\right) \sqrt{\omega\omega'} \sum_{\ell, m} \mathcal{S}_{\ell}^{\text{TE}-1}(k) \mathcal{S}_{\ell}^{\text{TE}-1}(k') \frac{(-1)^{\ell}}{kk'} \\ &\times \left\{ \ell(\ell+1) j_{\ell}(kR) j_{\ell}(k'R) + [kR j_{\ell}(kR)]' [k'R j_{\ell}(k'R)]' \right\} \\ &\times Y_{\ell}^m(\hat{\mathbf{k}}) Y_{\ell}^{m*}(\hat{\mathbf{k}}') , \end{aligned} \quad (3.21a)$$

$$\begin{aligned} \langle k_{\text{TM}}, k'_{\text{TM}}; R | \mathcal{F}_r | 0; R(\tau) \rangle &= \frac{n}{2\pi} \left(1 - \frac{1}{n^2}\right) \sqrt{\omega\omega'} \sum_{\ell, m} \mathcal{S}_{\ell}^{\text{TM}-1}(k) \mathcal{S}_{\ell}^{\text{TM}-1}(k') \frac{(-1)^{\ell}}{kk'} \\ &\times \left\{ kk'R^2 - \ell(\ell+1) \right\} j_{\ell}(kR) j_{\ell}(k'R) Y_{\ell}^m(\hat{\mathbf{k}}) Y_{\ell}^{m*}(\hat{\mathbf{k}}') , \end{aligned} \quad (3.21b)$$

$$\langle k_{\text{TM}}, k'_{\text{TM}}; R | \mathcal{F}_r | 0; R(\tau) \rangle = 0 , \quad (3.21c)$$

where the normalization constants $\mathcal{S}_\ell^{\text{TE},\text{TM}-1}(k)$ are as given in eqs. (B8) and (B9).

The probability of creating a photon pair in the mode $|k, k'\rangle$ from the initial vacuum state is given by the modulus square of the amplitude $c_{kk'}$, eq. (3.20), featuring the above matrix elements of the force operator. The state of the photon field is specified by eq. (3.12). Hence $c_{kk'}$ carries all information one needs to determine the expectation values of all interesting observables, especially the total radiated energy and the spectral density, which are the subject of the following section.

4 RADIATED ENERGY AND SPECTRAL DENSITY

As $|c_{kk'}(t)|^2$ is the probability of creating a photon pair in the mode $|k, k'\rangle$, the total energy of the photons radiated by the bubble interface during one acoustic cycle reads

$$\mathcal{W} = \frac{1}{2} \int_0^T dt \int_{-\infty}^{\infty} d^3\mathbf{k} \int_{-\infty}^{\infty} d^3\mathbf{k}' (\omega + \omega') |c_{kk'}(t)|^2, \quad (4.1)$$

where T is the period of the sound field. Inserting $c_{kk'}(t)$ from (3.20) and (3.21) one obtains for \mathcal{W}

$$\mathcal{W} = \frac{(n^2 - 1)^2}{8\pi^2 n^2} \int_0^\infty d\omega \int_0^\infty d\omega' \frac{\omega\omega'}{\omega + \omega'} \int_0^T d\tau \int_0^T d\tau' \beta(\tau)\beta(\tau') e^{i(\omega+\omega')(\tau-\tau')} \times \mathfrak{S}(k, k', R(\tau), R(\tau')), \quad (4.2)$$

with the auxiliary function \mathfrak{S} defined as

$$\begin{aligned} \mathfrak{S}(k, k', R(\tau), R(\tau')) &= \sum_{\ell=1}^{\infty} (2\ell + 1) \\ &\times \left\{ \mathcal{S}_\ell^{\text{TE}-1}(kR(\tau)) \mathcal{S}_\ell^{\text{TE}-1}(k'R(\tau)) \mathcal{S}_\ell^{\text{TE}* -1}(kR(\tau')) \mathcal{S}_\ell^{\text{TE}* -1}(k'R(\tau')) \right. \\ &\times \left[\ell(\ell + 1) j_\ell(kR(\tau)) j_\ell(k'R(\tau)) + [kR(\tau) j_\ell(kR(\tau))]' [k'R(\tau) j_\ell(k'R(\tau))] \right] \\ &\times \left[\ell(\ell + 1) j_\ell(kR(\tau')) j_\ell(k'R(\tau')) + [kR(\tau') j_\ell(kR(\tau'))]' [k'R(\tau') j_\ell(k'R(\tau'))]' \right] \\ &+ \mathcal{S}_\ell^{\text{TM}-1}(kR(\tau)) \mathcal{S}_\ell^{\text{TM}-1}(k'R(\tau)) \mathcal{S}_\ell^{\text{TM}* -1}(kR(\tau')) \mathcal{S}_\ell^{\text{TM}* -1}(k'R(\tau')) \\ &\times \left[kk'R^2(\tau) - \ell(\ell + 1) \right] \left[kk'R^2(\tau') - \ell(\ell + 1) \right] \\ &\times \left. j_\ell(kR(\tau)) j_\ell(k'R(\tau)) j_\ell(kR(\tau')) j_\ell(k'R(\tau')) \right\}, \quad (4.3) \end{aligned}$$

and the normalization factors $\mathcal{S}_\ell^{\text{TE},\text{TM}-1}(k)$ as given by eqs. (B8) and (B9).

A spectrometer measures the single-photon spectrum, which by symmetry is isotropic for a spherical bubble. The quantity of interest is therefore the angle-integrated spectral density radiated during one acoustic cycle,

$$\mathcal{P}(\omega) = \omega^3 \int_0^T dt \oint d\Omega_{\mathbf{k}} \int_{-\infty}^{\infty} d^3\mathbf{k}' |c_{kk'}(t)|^2, \quad (4.4)$$

which becomes

$$\mathcal{P}(\omega) = \frac{(n^2 - 1)^2}{4\pi^2 n^2} \omega^2 \int_0^\infty d\omega' \frac{\omega'}{(\omega + \omega')^2} \int_0^T d\tau \int_0^T d\tau' \beta(\tau)\beta(\tau') e^{i(\omega+\omega')(\tau-\tau')} \times \mathfrak{S}(k, k', R(\tau), R(\tau')). \quad (4.5)$$

The main difficulty in calculating the radiated energy \mathcal{W} and the spectrum $\mathcal{P}(\omega)$ is the evaluation of the auxiliary function \mathfrak{S} . To find an analytical approximation for \mathfrak{S} is a rather laborious task.

First, note that both \mathcal{W} and $\mathcal{P}(\omega)$, eqs. (4.2) and (4.5), contain a prefactor $(n^2 - 1)^2$ multiplying \mathfrak{S} , so that they vanish in the limit $n \rightarrow 1$, as they should; in this limit there is no dielectric interface to produce radiation. This justifies an expansion around $n = 1$ in \mathfrak{S} , which to first order does nothing but reduce the normalization factors $\mathcal{S}_\ell^{\text{TE, TM}^{-1}}$ in (4.3) to 1, by virtue of eq. (B10); otherwise \mathfrak{S} is independent of n .

In the present application the arguments of the Bessel functions in \mathfrak{S} are generally greater than 1, partly appreciably much greater, so that expansions for Bessel functions of small arguments are of no use here. As the summation over the index ℓ runs up to infinity, the sum will be dominated by terms for which argument and index of each of the Bessel functions are comparable in magnitude. Hence Debye's uniform asymptotic expansion has to be employed (cf. [26] formulae 9.3.3 and 9.3.7). So, for instance, one obtains in the regime $x \geq (\ell + 1/2)$

$$j_\ell(x) \longrightarrow \frac{1}{\nu} \frac{1}{\sqrt{\sec \beta \tan \beta}} \cos(\nu \tan \beta - \nu \beta - \frac{\pi}{4})$$

and

$$[x j_\ell(x)]' \longrightarrow -\sqrt{\frac{\tan \beta}{\sec \beta}} \sin(\nu \tan \beta - \nu \beta - \frac{\pi}{4}),$$

where the abbreviations $\nu \equiv (\ell + 1/2)$ and $x \equiv \nu \sec \beta$ have been introduced.

With the help of the above asymptotic approximations and by turning the summation over ℓ into an integration one can derive that \mathfrak{S} behaves approximately like $kk'R(\tau)R(\tau')$ in the short-wavelengths regime, i.e. when the photon wavelengths are shorter than the minimum bubble radius. Numerical investigation of the behaviour of \mathfrak{S} confirms this and yields

$$\mathfrak{S} \sim 1.16 kk'R(\tau)R(\tau'). \quad (4.6)$$

Employing this approximation one can integrate the expression (4.2) for \mathcal{W} and obtains after a short calculation:

$$\mathcal{W} = 1.16 \frac{(n^2 - 1)^2}{n^2} \frac{1}{480\pi} \int_0^T d\tau \frac{\partial^5 R^2(\tau)}{\partial \tau^5} R(\tau)\beta(\tau). \quad (4.7)$$

One of the interesting consequences of this result is that the dissipative force acting on the moving dielectric interface can be seen to behave like $R^2\beta^{(4)}(t)$ (+ terms with lower derivatives of β). This dependence tallies with results of calculations for frictional forces on moving perfect mirrors (see esp. [30]); the dissipative part of the radiation pressure on a moving dielectric or mirror is proportional to the fourth derivative of the velocity.

The expression (4.7) indicates also that any discontinuity in $\beta^{(3)}(t)$ or lower derivatives of β unavoidably leads to a divergence in \mathcal{W} (and also in the spectral density $\mathcal{P}(\omega)$). Especially, one is not permitted to assume a step-function profile for $R(t)$ during the collapse of the bubble, since this would give the physically meaningless result of infinite photon production, which is not salvageable by a cut-off or any other artificial regularization [13].

What produces the massive burst of photons from a collapsing sonoluminescent bubble is the turn-around of the velocity at the minimum radius of the bubble. There the velocity

rapidly changes sign, from collapse to re-expansion of the bubble. This means that the acceleration is peaked at this moment and so are higher derivatives of the velocity.

In order to estimate the total energy radiated during one acoustic cycle, one can use the approximation (4.6) to rewrite the expression (4.2) as

$$\mathcal{W} = 1.16 \frac{(n^2 - 1)^2}{960 \pi^2 n^2} \int_0^\infty d\Omega \Omega^4 \left| \int_0^T d\tau \frac{\partial R^2(\tau)}{\partial \tau} e^{i\Omega\tau} \right|^2 \quad (4.8)$$

where Ω is the sum of the photon frequencies in a pair. As \mathcal{W} is a functional of the time-dependent radius $R(t)$, one has to model $R(t)$ appropriately in order to be able to obtain a number for \mathcal{W} . At the collapse of the bubble the function $R(t)$ has a sharp dip; hence it is reasonable to adopt the model profile

$$R^2(t) = R_0^2 - (R_0^2 - R_{\min}^2) \frac{1}{(t/\gamma)^2 + 1} \quad (4.9)$$

for the time-dependence of the bubble radius. Figure 1 illustrates $R^2(t)$ for various values of the parameter γ which describes the timescale of the collapse and re-expansion process. The shorter γ the faster is the turn-around of the velocity at minimum radius and the more violent is the collapse. In the figure γ is half of the width of the dip halfway between R_0^2 and R_{\min}^2 . In this simple model the total radiated energy (4.8) reads in SI units

$$\mathcal{W} = 1.16 \frac{3(n^2 - 1)^2}{512 n^2} \frac{\hbar}{c^4 \gamma^5} (R_0^2 - R_{\min}^2)^2. \quad (4.10)$$

Experimental data on sonoluminescent bubbles [7] suggest that $R_0 \sim 10\mu\text{m}$ and $R_{\min} \sim 0.5\mu\text{m}$ are sensible values to assume. With $n \sim 1.3$ one obtains

$$\mathcal{W} = 1.8 \cdot 10^{-13} \text{ J for } \gamma \sim 1\text{fs}, \quad (4.11)$$

which corresponds roughly to the experimentally observed amount of energy per burst. Calculating the radiated spectral density in the same model gives

$$\mathcal{P}(\omega) = 1.16 \frac{(n^2 - 1)^2}{64 n^2} \frac{\hbar}{c^4 \gamma} (R_0^2 - R_{\min}^2)^2 \omega^3 e^{-2\gamma\omega}. \quad (4.12)$$

This is one of the most important end-results of this calculation, as it exhibits the same ω dependence as black-body radiation. Equating the exponent in (4.12) to $\hbar\omega/kT$ one derives that a turn-around time γ of 1fs corresponds to a temperature of around 4000K. This is however just a very crude estimate, as a lot of simplifications and approximations have been made in proceeding from (4.2) to (4.12); in general, the functional dependence of \mathcal{P} on ω will not be as simple, although its overall behaviour is as characterized by eq. (4.12).

The major problem in the above derivation is that the approximation (4.6) is good only at photon wavelengths that are smaller than the bubble radius R , i.e. when all products kR and $k'R$ are greater than 1. Once kR reaches down to the order of 1 or even below, one has to expect resonances of the photon wavelengths with the bubble radius. An exploration of any such resonance effects requires taking into account the full kR dependence of the auxiliary integral \mathfrak{S} in eq. (4.3), which is fairly difficult even numerically.

The results of a computer simulation of a model like the one specified by (4.9) with $R_0 = 45\mu\text{m}$, $R_{\min} = 3\mu\text{m}$, and $\gamma = 10\text{fs}$ are shown in figures 2 and 3. Comparing these with the values of \mathcal{P} predicted by eq. (4.12), one sees that the numerical results show an enhancement of about a factor 1000 in \mathcal{P} relative to the analytical approximation. This is due to resonant behaviour in (4.9), since R_{\min} is not any more appreciably much larger than the wavelength of the observed light. Numerical studies in the regime $kR_{\min} \lesssim 1$ are hindered by substantial expense in computation time; work by the present author is in progress [31]. One can expect to see an even greater enhancement in \mathcal{P} over the predictions of eq. (4.12) for what are believed to be realistic values of R_{\min} , i.e. values around $0.5\mu\text{m}$. Thus, one can presumably substantially relax the requirement on how small the turn-around time γ between collapse and re-expansion of the bubble has to be in order for the present theory to yield the experimentally observed number of photons. The crude model that led to the estimate (4.11) would demand γ to be as short as 1fs, if it were to account for the experimental data for the sonoluminescence of an air bubble in water. The numerical calculation resulting in the figures 2 and 3 suggests that $\gamma \sim 10\text{fs}$ is fully sufficient; calculations for R_{\min} smaller than $3\mu\text{m}$ will most likely require merely $\gamma \sim 100\text{fs} \dots 10\text{ps}$, which is closer to what one expects this timescale to be on physical grounds.

The features seen in the spectrum in figure 2 seem to be due to resonances between photon wavelengths and bubble size, but again, extensive numerical studies are needed to explore them [31]. Comparison of the figures 2 and 3 makes it very clear that plotting data over photon wavelength rather than frequency tends to conceal such features; it might therefore be beneficial to plot experimental data over photon frequency as well.

Given the time-dependence of the bubble radius $R(t)$, one can in principle, technical difficulties aside, predict the sonoluminescence spectrum radiated by the bubble from eqs. (4.5) and (4.3). The next section summarizes the questions answered by the theory of quantum vacuum radiation and spells out some of the as yet unanswered ones.

5 SUMMARY AND CRITICAL REFLECTION

5.1 Successfully resolved issues

5.1.1 Results for the spectral density and restrictions on the turn-around time γ

The results of the previous section seem in concord with the experimentally observed facts in sonoluminescence. Knowing the time-dependence of the bubble radius $R(t)$ one can evaluate the radiated spectral density from eqs. (4.5) and (4.3). The analytical estimate (4.11) for the total energy radiated during one acoustic cycle and the results of numerical calculations presented in figs. 2 and 3 show good qualitative and quantitative agreement with the experimental data [5]. The function $R(t)$ has been modelled by a dip, as written down in eq. (4.9) and made visual in fig. 1. The width of this dip is characterized by the important parameter γ , whose physical significance is that it is a measure of the time-scale of the turn-around of the velocity between the collapse and the re-expansion of the bubble. To model the experimentally observed data on the basis of the numerical calculations worked through so far, this turn-around has to happen in about 10fs. Further numerical

analysis of eqs. (4.5) and (4.3) in the regime where the radiated photon wavelengths get in resonance with the bubble size can be anticipated to relax this requirement to a turn-around time of roughly 100fs...10ps, which seems quite realistic. Unfortunately, it is notoriously difficult to determine γ experimentally, as it is arduous to measure the bubble radius close to the collapse; the laser light that is used to determine the bubble radius by means of fitting the scattering data to the Mie theory, is then most likely reflected by the shock-wave front propagating through the water rather than by the actual bubble surface [7]. In addition, one might also have to take into account that the bubble shape deviates, perhaps even substantially, from spherical. Although this does not affect the present theory of the radiation mechanism to any discernible extent, since the spectrum of the vacuum fluctuations is known to be affected by the shape only to higher order [33], it will noticeably alter the light-scattering properties so that the Mie scattering theory is no longer applicable. Nevertheless, the currently available experimental data seem to suggest that γ lies somewhere in the interval 100fs...10ps[7].

5.1.2 Thermal properties of the spectral density

The similarity of the observed photon spectrum to a black-body spectrum has its origin in the fact that the photon radiation emerges in coherent pairs. To obtain the single-photon spectrum, which is the one measured in spectral analyses, one has to trace over one photon in the pair, as done by integrating over k' in eq. (4.4). This process of tracing is known to engender thermal properties of the single-photon spectrum, even though the original two-photon state was a pure state and one has dealt with zero-temperature quantum field theory throughout [21]. In other words, it is the particular correlations within the radiated photon pairs that engender the thermal-like properties of the spectrum, and thermal processes are completely independent of this and in the case of sonoluminescence presumably of no significance whatsoever.

5.1.3 Features in the spectrum

Features in the otherwise smooth experimental spectra can be explained by a combination of three things:

(i) Resonance effects in the radiation mechanism occur when the size of the bubble $R(t)$ and the photon wavelengths λ are of the same order of magnitude. The features seen in the numerically calculated spectral density in figure 2 are due to higher-order resonances of this kind where the R is an integer multiple of λ ; for direct resonances one expects much stronger effects. General predictions for such features can hardly be made as their detailed qualities are determined by the time-dependence of R , which leads over to the next point.

(ii) Choosing gases other than air for the bubble contents leads to a modified dynamics of the bubble surface, as gas solubilities in water vary; but even a slightly different $R(t)$ around the collapse will change the structure of the resonance effects between λ and R , which is why one expects a strong dependence of the sonoluminescence spectra on the gas that saturates the water, as indeed observed in experiments [11, 32].

(iii) The experimentally seen features in the spectrum might just as well be caused by dispersion, i.e. the dependence of the refractive index n on the photon frequency ω . As long as n depends only weakly on ω , one can replace n by $n(\omega)$ in eqs. (4.5) and (4.12) by virtue of

adiabaticity. This explains that the experimental data show features at frequencies close to the vibration-rotation excitations of the water molecule [9]. Especially, one can expect this to be the dominant effect in the spectra of multi-bubble sonoluminescence, as the resonances discussed under (i) above will average out if bubbles grow and collapse in a random manner.

5.1.4 Predicted pulse length

Apart from predicting the radiated spectrum, the theory of quantum vacuum radiation solves several conceptual problems that previous theories have not been able to deal with satisfactorily. Most importantly, the present theory has no difficulty in explaining the extreme shortness of the emitted light pulses; their duration is determined by the parameter γ describing the turn-around time at the collapse and the time it takes for the fluctuations to correlate around the bubble. As the latter is on the scale of merely one or a few femtoseconds, γ is the decisive quantity. Thus one expects the pulse length to lie between 100fs and 10ps, which tallies with the experimental observations.

5.1.5 Absence of radiation in the UV

Another major question that is successfully answered by the present theory concerns the absence of radiation below the absorption edge of water at around 180nm. Water has essentially no polarizability below this wavelength, so that the real part of its refractive index is very close to 1. Hence the mechanism of exciting vacuum fluctuations into real photon pairs is inoperative below 180nm; no radiation is emitted and no radiation has to be re-absorbed. This explains the absence of any macroscopically discernible effect on the water by the large amounts of absorbed light predicted by theories of black-body radiation or bremsstrahlung (cf. Sec. I A).

5.2 Suggested experiments

Thinking about experiments that distinguish the present from other theories of sonoluminescence, one quickly comes up with two relatively simple ones. One is to look for photons emitted in the X-ray transparency window of water [34]; both the black-body and the bremsstrahlung theories predict a perceptible amount of photons with wavelengths of around 1\AA , whereas the present theory denies any photon emission at such short wavelengths since the polarizability of water is essentially zero for X-rays, i.e. $(n - 1) \approx 0$.

The second presumably easily set up experiment is to force the bubble into an elongated rather than spherical shape by using piezoelectric transducers on two or all three axes and to examine the angular distribution of the emitted light. For such a case the present theory, unlike others, predicts an anisotropic intensity; the number of photons radiated into a given direction is roughly proportional to the cross-section of the bubble perpendicular to that direction. Thus, if the bubble is spheroidal rather than spherical during the radiation process, one expects anisotropy.

5.3 Agenda and open questions

The most important point still to be attended to is to extend the numerical calculations of the spectral density (4.5) down to realistic minimum bubble sizes of one micron or less [31]. This will allow one to make more precise statements as to the turn-around time γ required to produce the experimentally observed number of photons (cf. Sec. A 1) and to explore the effects of resonances if the bubble size is comparable to the photon wavelengths (cf. Sec. A 3).

Another effect to be studied in detail is the photon radiation produced by the rapid variation of the refractive index of water due to the rapidly varying compression around the outside of the bubble [31]. Preliminary estimations have shown that this mechanism is of secondary importance for the sonoluminescence problem; to understand the principle of it might, however, be useful in view of other applications.

An academic, but nevertheless interesting question to ask is where the photons actually are produced. A model calculation for a one-dimensional moving dielectric filling a half-space [18] has indicated that, although the emission of this kind of quantum vacuum radiation depends on the existence of a moving interface between two media of different refractive indices, the photons do not come directly from the interface but from within a certain vicinity of it, as suggested also by physical intuition. However, inconsistencies between where the photons are produced and which the support of the radiation pressure on the dielectric is, are buried in the assumption of a perfectly rigid dielectric.

The hydrodynamics of the bubble has been considered as given in the present work; its theory has been quite successfully established [6]. However, especially in view of relaxing restrictions on the velocity and the acceleration of the bubble surface in that theory and of scrutinizing the bubble dynamics at the moment of collapse, the important role of the back-reaction of the photon radiation onto the bubble should be recognized. The momentum loss due to the radiation process might have a significant effect on the bubble. While the emission lasts the equations motion of the liquid-gas interface will be supplemented by a frictional force which is roughly proportional to the fourth derivative of the velocity of the interface, as discussed just below eq. (4.7).

One of the puzzles that remain is why stable single-bubble sonoluminescence is seen only in water, although multi-bubble sonoluminescence has been observed in a variety of fluids. The present author's conjecture is that the reason for this is buried in the unusual properties of gas solubility of water, which conspire with hydrodynamic mechanisms to lead to an exceptionally sharp and violent collapse of a driven bubble. In other fluids such conditions might be reached at random, but not in a regular fashion to produce radiation from stably maintained bubbles.

5.4 Credo

To close a conceptual remark might be appropriate. At first sight, the idea that the burst of photons seen in sonoluminescence has its origin in the zero-point fluctuations of the electromagnetic field might seem utterly strange, as one tends to think of low-energy photons emitted from material media as coming from atomic transitions. Pondering on this, one has to admit that all we really know is that photons come from some kind of moving charge

or, field-theoretically speaking, from the coupling to a fermion field. As we structure our thinking, we are most inclined to consider atoms as the basic entities of all materials and try to explain all physical phenomena on this basis. However, there is no reason for so doing; we are completely at liberty to mentally re-group these charges in a variety of different ways and should choose whichever is most appropriate for the problem at hand. In the case of sonoluminescence atoms are obviously not the basic entities to be considered, since atomic transitions are about a thousand times slower than a sonoluminescence pulse. Here the basic structure of the medium with respect to the radiation process is most suitably thought of as an assembly of dipoles with a certain dielectric response. This point of view enables one to consider the cooperative response of the charges to the zero-point fluctuations of the electromagnetic field, and quantum vacuum radiation emerges as a consequence quite naturally.

ACKNOWLEDGMENTS

It is a pleasure to thank Peter W. Milonni for drawing my attention to the phenomenon of sonoluminescence, for pointing out to me Julian Schwinger's thought that this might relate to the zero-point fluctuations of the photon field, and for urging me to apply my knowledge from the theory of moving dielectrics to this problem. Furthermore, I am grateful to Peter L. Knight for telling me about the apparent thermal properties of pure two-mode states when traced over one of the photons, and I would like to thank Gabriel Barton, Nigel D. Goldenfeld, Anthony J. Leggett, Efrat Shimshoni, and Shivaji L. Sondhi for their interest, stimulating discussions, and many questions. I have also benefited from a discussion with Paul M. Goldbart about the completeness of spherical solutions of the wave equation. Financial support through the John D. and Catherine T. MacArthur Foundation is gratefully acknowledged.

APPENDIX A: HAMILTONIAN FOR A DIELECTRIC IN UNIFORM MOTION

The standard way of deriving a Hamiltonian is to proceed from a Lagrangian density. The Lagrangian density for a homogeneous dielectric moving rigidly and uniformly is a function of the dielectric constant ε of the medium and of the velocity β of the medium relative to the frame of the observer;

$$\mathcal{L} = \mathcal{L}(\varepsilon, \beta) .$$

It is uniquely determined by the following three requirements:

(i) In the limit of $\beta = 0$ it should reduce to the familiar Lagrangian density for a stationary dielectric

$$\mathcal{L}(\varepsilon, \beta=0) = \frac{1}{2} \left(\frac{\mathbf{D}^2}{\varepsilon} - \mathbf{B}^2 \right) . \quad (\text{A1})$$

(ii) For an optically transparent medium one should recover the Lagrangian density of the vacuum, which, by Lorentz invariance, is independent of the velocity β ;

$$\mathcal{L}(\varepsilon=1, \beta) = -\frac{1}{4} F_{\mu\nu} F^{\mu\nu} = \frac{1}{2} (\mathbf{E}^2 - \mathbf{B}^2) . \quad (\text{A2})$$

The symbol $F_{\mu\nu}$ denotes the field strength tensor of the electromagnetic field, $F_{\mu\nu} = \nabla_\mu A_\nu - \nabla_\nu A_\mu$. Its dual is defined $\tilde{F}_{\mu\nu} = 1/2 \epsilon_{\mu\nu\alpha\beta} F^{\alpha\beta}$.

(iii) \mathcal{L} must be a Lorentz scalar. The only true scalars that are quadratic in the fields and that depend solely on the field strength $F_{\mu\nu}$ and on the four-velocity u_μ of the medium are $F_{\mu\nu} F^{\mu\nu}$, $u_\mu F^{\mu\nu} u^\alpha F_{\alpha\nu}$, and $u_\mu \tilde{F}^{\mu\nu} u^\alpha \tilde{F}_{\alpha\nu}$.

From the above the Lagrangian density is found to be

$$\mathcal{L}(\varepsilon, \beta) = -\frac{1}{4} F_{\mu\nu} F^{\mu\nu} - \frac{\varepsilon - 1}{2} u_\mu F^{\mu\nu} u^\alpha F_{\alpha\nu} . \quad (\text{A3})$$

Now the Hamiltonian can be derived by going through the canonical formalism

$$\mathbf{\Pi} = \frac{\delta \mathcal{L}}{\delta \dot{\mathbf{A}}} , \quad (\text{A4a})$$

$$\mathcal{H} = \mathbf{\Pi} \cdot \dot{\mathbf{A}} - \mathcal{L} . \quad (\text{A4b})$$

This leads to the Hamiltonian density

$$\mathcal{H} = \frac{1}{2} \frac{\varepsilon(1 - \beta^2)}{\varepsilon - \beta^2} \left(\frac{\mathbf{\Pi}^2}{\varepsilon} + \mathbf{B}^2 \right) - \frac{\varepsilon - 1}{\varepsilon - \beta^2} \beta \cdot (\mathbf{\Pi} \wedge \mathbf{B}) + \frac{1}{2} \frac{\varepsilon - 1}{\varepsilon - \beta^2} \left[\frac{(\beta \cdot \mathbf{\Pi})^2}{\varepsilon} + (\beta \cdot \mathbf{B})^2 \right] . \quad (\text{A5})$$

Substituting $\mathbf{\Pi} = -\mathbf{D}$ and, with a perturbative treatment in mind, expanding in powers of the velocity β , one obtains

$$H = \int d^3\mathbf{r} \left[\frac{1}{2} \left(\frac{\mathbf{D}^2}{\varepsilon} + \mathbf{B}^2 \right) + \frac{\varepsilon - 1}{\varepsilon} \beta \cdot (\mathbf{D} \wedge \mathbf{B}) + \mathcal{O}(\beta^2) \right] . \quad (\text{A6})$$

This is a very natural result; the Hamiltonian for a stationary dielectric is augmented by an energy-fluxlike correction which vanishes for a transparent medium.

Another way of arriving at the same result is to appeal to the Lorentz invariance of the Maxwell theory. The Hamiltonian density must in any frame be given by

$$\mathcal{H} = \frac{1}{2} (\mathbf{D} \cdot \mathbf{E} + \mathbf{B} \cdot \mathbf{H}) , \quad (\text{A7})$$

where the fields are as measured in this frame. For a non-magnetic dielectric $\mathbf{B} = \mathbf{H}$, but the \mathbf{D} and \mathbf{E} fields are connected by some non-trivial constitutive relation which can be found by Lorentz-transforming the constitutive relation $\mathbf{D}' = \varepsilon \mathbf{E}'$ valid in the rest-frame of the medium into the laboratory frame. There the constitutive relations read

$$\mathbf{E}_{\parallel} = \frac{1}{\varepsilon} \mathbf{D}_{\parallel} , \quad (\text{A8a})$$

$$\mathbf{E}_{\perp} = \frac{\varepsilon}{\varepsilon - \beta^2} \left[\frac{1}{\varepsilon} (1 - \beta^2) \mathbf{D}_{\perp} - \frac{\varepsilon - 1}{\varepsilon} \beta \wedge \mathbf{B} \right] . \quad (\text{A8b})$$

Utilizing these to replace \mathbf{E} and \mathbf{H} in eq (A7) one recovers the Hamiltonian density (A5) obtained earlier by different means.

APPENDIX B: MODE EXPANSION FOR THE HELMHOLTZ EQUATION IN SPHERICAL COORDINATES

The mode functions $A_{(1,2)}^{\text{TE},\text{TM}}$ in the expansions (2.7) are solutions of the Helmholtz equation

$$\omega^2 \varepsilon(\mathbf{r}) \mathbf{A}(\mathbf{r}, \mathbf{k}) + \nabla^2 \mathbf{A}(\mathbf{r}, \mathbf{k}) = 0, \quad \omega = |\mathbf{k}|. \quad (\text{B1})$$

Rewriting this equation as

$$\left(\frac{1}{\sqrt{\varepsilon}} \nabla^2 \frac{1}{\sqrt{\varepsilon}} \right) \sqrt{\varepsilon} \mathbf{A} = -\omega^2 \sqrt{\varepsilon} \mathbf{A} \quad (\text{B2})$$

makes obvious that this is the eigenvalue equation of the Hermitean operator $(1/\sqrt{\varepsilon})\nabla^2(1/\sqrt{\varepsilon})$, and hence the mode functions $\sqrt{\varepsilon}\mathbf{A}$ form a complete set of orthogonal functions.

In order to diagonalize the Hamiltonian (2.1) into the Hamiltonian (2.6) of the photon field by means of the mode expansions (2.7), the mode functions should satisfy the orthonormalization conditions

$$\int d^3\mathbf{r} \varepsilon(\mathbf{r}) \left[\mathbf{A}_{(1)}^{\text{TE},\text{TM}}(\mathbf{r}; \mathbf{k}) \mathbf{A}_{(1)}^{\text{TE},\text{TM}*}(\mathbf{r}; \mathbf{k}') + \mathbf{A}_{(2)}^{\text{TE},\text{TM}}(\mathbf{r}; \mathbf{k}) \mathbf{A}_{(2)}^{\text{TE},\text{TM}*}(\mathbf{r}; \mathbf{k}') \right] = \delta^{(3)}(\mathbf{k} - \mathbf{k}') \quad (\text{B3})$$

for each the TE and the TM polarizations.

To find the solutions of the Helmholtz equation (B1) one conveniently proceeds from the scalar solution

$$\Phi = \frac{4\pi}{(2\pi)^{3/2}} \sum_{\ell,m} e^{-i\delta_\ell} i^\ell [\cos \delta_\ell j_\ell(nkr) + \sin \delta_\ell y_\ell(nkr)] Y_\ell^{m*}(\hat{\mathbf{k}}) Y_\ell^m(\hat{\mathbf{r}}) \quad (\text{B4})$$

which is normalized to behave like a plane wave $e^{i\mathbf{k}\cdot\mathbf{r}}/(2\pi)^{3/2}$ for $kr \rightarrow \infty$. The phase δ_ℓ will be chosen to meet the required continuity conditions across the surface of the bubble.

The vector field operators invariant under rotation are \mathbf{r} , ∇ , $\mathbf{L} = -i\mathbf{r} \times \nabla$, and $\nabla \times \mathbf{L}$. Since \mathbf{r} fails to commute with ∇^2 , only the last three operators may be used to generate rotation-invariant vector solutions of the Helmholtz equation. However, $\nabla\Phi$ is an irrotational field; only the solenoidal fields $\mathbf{L}\Phi$ and $(\nabla \times \mathbf{L})\Phi$ can be employed for representations of the transversely polarized electromagnetic field. Choosing $\mathbf{A}_{(1)} \sim \mathbf{L}\Phi$ and $\mathbf{A}_{(2)} \sim 1/(nk) \nabla \times \mathbf{L}\Phi$ and observing the correct normalization (B3) one obtains for the mode functions outside the

bubble

$$\begin{aligned}
A_{(1)\theta} &= \sqrt{\frac{\bar{n}}{\pi}} \sum_{\ell,m} \frac{e^{-i\delta_\ell} i^\ell}{\sqrt{\ell(\ell+1)}} [\cos \delta_\ell j_\ell(nkr) + \sin \delta_\ell y_\ell(nkr)] Y_\ell^{m*}(\hat{\mathbf{k}}) \frac{(-m)}{\sin \theta} Y_\ell^m(\hat{\mathbf{r}}), \\
A_{(1)\varphi} &= \sqrt{\frac{\bar{n}}{\pi}} \sum_{\ell,m} \frac{e^{-i\delta_\ell} i^\ell}{\sqrt{\ell(\ell+1)}} [\cos \delta_\ell j_\ell(nkr) + \sin \delta_\ell y_\ell(nkr)] Y_\ell^{m*}(\hat{\mathbf{k}}) (-i) \frac{\partial Y_\ell^m(\hat{\mathbf{r}})}{\partial \theta}, \\
A_{(1)r} &= 0, \\
A_{(2)\theta} &= \sqrt{\frac{\bar{n}}{\pi}} \sum_{\ell,m} \frac{e^{-i\delta_\ell} i^\ell}{\sqrt{\ell(\ell+1)}} \frac{1}{nkr} [nkr \cos \delta_\ell j_\ell(nkr) + nkr \sin \delta_\ell y_\ell(nkr)]' \\
&\quad \times Y_\ell^{m*}(\hat{\mathbf{k}}) i \frac{\partial Y_\ell^m(\hat{\mathbf{r}})}{\partial \theta}, \\
A_{(2)\varphi} &= \sqrt{\frac{\bar{n}}{\pi}} \sum_{\ell,m} \frac{e^{-i\delta_\ell} i^\ell}{\sqrt{\ell(\ell+1)}} \frac{1}{nkr} [nkr \cos \delta_\ell j_\ell(nkr) + nkr \sin \delta_\ell y_\ell(nkr)]' \\
&\quad \times Y_\ell^{m*}(\hat{\mathbf{k}}) \frac{(-m)}{\sin \theta} Y_\ell^m(\hat{\mathbf{r}}), \\
A_{(2)r} &= \sqrt{\frac{\bar{n}}{\pi}} \sum_{\ell,m} \frac{e^{-i\delta_\ell} i^\ell}{\sqrt{\ell(\ell+1)}} \frac{i\ell(\ell+1)}{nkr} [\cos \delta_\ell j_\ell(nkr) + \sin \delta_\ell y_\ell(nkr)] Y_\ell^{m*}(\hat{\mathbf{k}}) Y_\ell^m(\hat{\mathbf{r}}),
\end{aligned} \tag{B5}$$

and for those inside the bubble

$$\begin{aligned}
A_{(1)\theta} &= \sqrt{\frac{\bar{n}}{\pi}} \sum_{\ell,m} \mathcal{S}_\ell^{-1} \frac{i^\ell}{\sqrt{\ell(\ell+1)}} j_\ell(kr) Y_\ell^{m*}(\hat{\mathbf{k}}) \frac{(-m)}{\sin \theta} Y_\ell^m(\hat{\mathbf{r}}), \\
A_{(1)\varphi} &= \sqrt{\frac{\bar{n}}{\pi}} \sum_{\ell,m} \mathcal{S}_\ell^{-1} \frac{i^\ell}{\sqrt{\ell(\ell+1)}} j_\ell(kr) Y_\ell^{m*}(\hat{\mathbf{k}}) (-i) \frac{\partial Y_\ell^m(\hat{\mathbf{r}})}{\partial \theta}, \\
A_{(1)r} &= 0, \\
A_{(2)\theta} &= \sqrt{\frac{\bar{n}}{\pi}} \sum_{\ell,m} \mathcal{S}_\ell^{-1} \frac{i^\ell}{\sqrt{\ell(\ell+1)}} \frac{1}{kr} [kr j_\ell(kr)]' Y_\ell^{m*}(\hat{\mathbf{k}}) i \frac{\partial Y_\ell^m(\hat{\mathbf{r}})}{\partial \theta}, \\
A_{(2)\varphi} &= \sqrt{\frac{\bar{n}}{\pi}} \sum_{\ell,m} \mathcal{S}_\ell^{-1} \frac{i^\ell}{\sqrt{\ell(\ell+1)}} \frac{1}{kr} [kr j_\ell(kr)]' Y_\ell^{m*}(\hat{\mathbf{k}}) \frac{(-m)}{\sin \theta} Y_\ell^m(\hat{\mathbf{r}}), \\
A_{(2)r} &= \sqrt{\frac{\bar{n}}{\pi}} \sum_{\ell,m} \mathcal{S}_\ell^{-1} \frac{i^\ell}{\sqrt{\ell(\ell+1)}} \frac{i\ell(\ell+1)}{kr} j_\ell(kr) Y_\ell^{m*}(\hat{\mathbf{k}}) Y_\ell^m(\hat{\mathbf{r}}).
\end{aligned} \tag{B6}$$

Here and in the following a prime behind a bracket means a derivative with respect to the argument of the spherical Bessel function. The mode functions for the inside of the bubble have zero phase shift because the fields have to be regular at the origin $r = 0$, which excludes any contributions from the spherical Bessel functions of the second kind y_ℓ as these diverge for zero argument.

The phase shifts $\delta_\ell^{\text{TE,TM}}$ and the normalization constants $\mathcal{S}_\ell^{\text{TE,TM}-1}$ are determined by the continuity conditions (2.4) across the bubble surface at $r = R$. One obtains

$$\tan \delta_\ell^{\text{TE}} = \frac{\mathcal{N}_\ell^{\text{TE}}}{\mathcal{D}_\ell^{\text{TE}}}, \quad \tan \delta_\ell^{\text{TM}} = \frac{\mathcal{N}_\ell^{\text{TM}}}{\mathcal{D}_\ell^{\text{TM}}}, \tag{B7}$$

and

$$\mathcal{S}_\ell^{\text{TE}-1} = \frac{1}{(nkR)} \frac{1}{(-\mathcal{D}_\ell^{\text{TE}} - i\mathcal{N}_\ell^{\text{TE}})}, \quad \mathcal{S}_\ell^{\text{TM}-1} = \frac{1}{(kR)} \frac{1}{(-\mathcal{D}_\ell^{\text{TM}} - i\mathcal{N}_\ell^{\text{TM}})}, \quad (\text{B8})$$

where

$$\begin{aligned} \mathcal{N}_\ell^{\text{TE}} &= j_\ell(kR) [nkR j_\ell(nkR)]' - j_\ell(nkR) [kR j_\ell(kR)]', \\ \mathcal{D}_\ell^{\text{TE}} &= y_\ell(nkR) [kR j_\ell(kR)]' - j_\ell(kR) [nkR y_\ell(nkR)]', \\ \mathcal{N}_\ell^{\text{TM}} &= j_\ell(kR) [nkR j_\ell(nkR)]' - n^2 j_\ell(nkR) [kR j_\ell(kR)]', \\ \mathcal{D}_\ell^{\text{TM}} &= n^2 y_\ell(nkR) [kR j_\ell(kR)]' - j_\ell(kR) [nkR y_\ell(nkR)]'. \end{aligned} \quad (\text{B9})$$

Note that

$$\lim_{n \rightarrow 1} \mathcal{S}_\ell^{\text{TE, TM}-1} = 1, \quad (\text{B10})$$

due to the fact that in this limit the $\mathcal{D}_\ell^{\text{TE, TM}}$ are simplified by the Wronskian of the spherical Bessel functions

$$j_\ell(x)y_\ell'(x) - j_\ell'(x)y_\ell(x) = \frac{1}{x^2},$$

and the $\mathcal{N}_\ell^{\text{TE, TM}}$ obviously reduce to zero.

APPENDIX C: FORCE ON A STATIONARY DIELECTRIC

There are several ways of deriving an expression for the force applied by an electromagnetic field on a dielectric body; the physically most intuitive one is to consider the force as ensuing from induced currents and surface-charge densities.

In Lorentz gauge or in Coulomb gauge without free charges the vector potential satisfies the wave equation

$$\frac{\partial}{\partial t} (\varepsilon \dot{\mathbf{A}}) - \nabla^2 \mathbf{A} = 0. \quad (\text{C1})$$

On rewriting this equation as

$$\ddot{\mathbf{A}} - \nabla^2 \mathbf{A} = \mathbf{j}_{\text{ind}},$$

one obtains an induced current density

$$\mathbf{j}_{\text{ind}} = -(\varepsilon - 1)\ddot{\mathbf{A}}. \quad (\text{C2})$$

By continuity

$$\frac{\partial \rho_{\text{ind}}}{\partial t} + \nabla \cdot \mathbf{j}_{\text{ind}} = 0$$

one finds that the induced surface-charge density is

$$\rho_{\text{ind}} = -\nabla \cdot \left(\frac{\varepsilon - 1}{\varepsilon} \mathbf{D} \right). \quad (\text{C3})$$

Therefore a stationary dielectric is acted upon by a force density

$$\mathbf{f} = \rho_{\text{ind}} \mathbf{E} + \mathbf{j}_{\text{ind}} \wedge \mathbf{B}. \quad (\text{C4})$$

On integrating this density over a dielectric with a cavity one has to bear in mind that the radial component of the electric field is not continuous across the boundary. However, the gradient of $(\varepsilon - 1)/\varepsilon$ in (C3) brings about a δ function on the surface of the cavity, which is multiplied by the electric field in eq (C4) for the force density. The mathematically and physically correct prescription is to substitute the electric field by the average of its values on the two sides of the boundary. Then one obtains for the radial component of the force on a spherical bubble of radius R

$$\mathcal{F}_r = - \left(1 - \frac{1}{n^2}\right) \frac{R^2}{2} \oint d\Omega \left[\left(1 + \frac{1}{n^2}\right) D_r^2 + B_r^2 - B_\theta^2 - B_\phi^2 \right], \quad (\text{C5})$$

where the integral runs over the complete solid angle; the tangential components of the force are zero as obvious from symmetry.

Strictly speaking, the expression (C5) is of course the force on the dielectric and not the force on the bubble. Nevertheless, since the two are complementary and the force density has δ -support on the boundary, i.e. the force is really applied only to the interface, it seems reasonable to speak of the force as acting on the bubble.

Another, less palpable and more formal way of calculating the force density (C4) is to proceed from the stress-energy-momentum tensor of the electromagnetic field. In this approach care must be taken when interpreting formulae, because the momentum density of the photon field in a dielectric medium is subject to ambiguity. However, this issue will not be addressed here as the force density is unequivocally defined and interpretable.

The stress exerted by the fields alone, i.e. the fields as in vacuum and exclusive of the polarization fields inside the dielectric, is given by the space-like components of the stress-energy-momentum tensor in vacuum

$$T_{(0)}^{ij}(\varepsilon=1) = -E_i E_j - B_i B_j + \frac{1}{2} \delta_{ij} (\mathbf{E}^2 + \mathbf{B}^2). \quad (\text{C6})$$

In vacuum there is no doubt about the momentum density carried by the field; it reads

$$T_{(0)}^{i0}(\varepsilon=1) = \epsilon_{ijk} E_j B_k, \quad (\text{C7})$$

which is just the Poynting vector. Overall momentum balance requires that the change in the mechanical momentum density of the material (i.e. the force density on the dielectric) together with the change in the momentum of the fields alone (C7) equal the negative gradient of the stress (C6) due to the fields,

$$\frac{\partial}{\partial t} \left[\mathcal{M}_{\text{mech}}^i + T_{(0)}^{i0}(\varepsilon=1) \right] = -\nabla_j T_{(0)}^{ij}(\varepsilon=1).$$

Thus the force density is given by

$$f_i = \frac{\partial \mathcal{M}_{\text{mech}}^i}{\partial t} = -\frac{\partial}{\partial t} T_{(0)}^{i0} - \nabla_j T_{(0)}^{ij}.$$

A few trivial transformations taking into account vector identities and the Maxwell equations yield

$$f_i = \left(1 - \frac{1}{\varepsilon}\right) \left(B_k \nabla_k B_i - \frac{1}{2} \nabla_i \mathbf{B}^2 \right) + E_i \nabla_j E_j.$$

Upon integration over the bubble the first part of this expression is easily seen to lead to the B -dependent terms in the force (C5). In order to recognize the second part one should note that $\nabla_j E_j \equiv \nabla \cdot \mathbf{E}$ is zero inside as well as outside the dielectric, but non-zero at the interface; $\nabla_j E_j$ gives a δ function on the surface multiplied by the difference of the outer and the inner electric fields. Thus one recovers the induced surface-charge density (C3), the force on which engenders the same D_r -dependent term as in (C5) before.

References

- [1] H. Frenzel and H. Schultes, Z. Phys. Chem., Abt. B **27**, 421 (1934).
- [2] D. F. Gaitan, L. A. Crum, C. C. Church, and R. A. Roy, J. Acoust. Soc. Am. **91**, 3166 (1992).
- [3] B. P. Barber and S. J. Putterman, Nature **352**, 318 (1991); B. P. Barber, R. Hiller, K. Arisaka, H. Fetterman, and S. J. Putterman, J. Acoust. Soc. Am. **91**, 3061 (1992).
- [4] R. G. Holt, D. F. Gaitan, A. A. Atchley, and J. Holzfuss, Phys. Rev. Lett. **72**, 1376 (1994).
- [5] R. Hiller, S. J. Putterman, and B. P. Barber, Phys. Rev. Lett. **69**, 1182 (1992).
- [6] R. Löfstedt, B. P. Barber, and S. J. Putterman, Phys. Fluids A **5**, 2911 (1993).
- [7] B. P. Barber and S. J. Putterman, Phys. Rev. Lett. **69**, 3839 (1992).
- [8] C. C. Wu and P. H. Roberts, Proc. R. Soc. Lond. A **445**, 323 (1994).
- [9] K. S. Suslick (private communication).
- [10] E. B. Flint and K. S. Suslick, Science **253**, 1397 (1991); and references therein.
- [11] Y. T. Didenko, T. V. Gordeychuk, and V. L. Koretz, J. Sound Vibr. **147**, 409 (1991).
- [12] L. Frommhold and A. A. Atchley, Phys. Rev. Lett. **73**, 2883 (1994).
- [13] J. Schwinger, Proc. Natl. Acad. Sci. USA **89**, 4091 (1992); **89**, 11118 (1992); **90**, 958 (1993); **90**, 2105 (1993); **90**, 4505 (1993).
- [14] H. B. G. Casimir, Proc. K. Ned. Akad. Wet. **51**, 793 (1948).
- [15] P. W. Milonni, *The Quantum Vacuum* (Academic, New York, 1994).
- [16] W. G. Unruh, Phys. Rev. **D 14**, 870 (1976).
- [17] N. D. Birrell and P. C. W. Davies, *Quantum Fields in Curved Space* (Cambridge University Press, 1982).
- [18] G. Barton and C. Eberlein, Ann. Phys. (N.Y.) **227**, 222 (1993).

- [19] In this way mean-square deviations of Casimir forces have been calculated for an infinite plane mirror by G. Barton, *J. Phys. A: Math. Gen.* **24**, 991 (1991); and for mirrors of finite size such as spheres and circular disks by C. Eberlein [33].
- [20] C. Eberlein, *J. Phys. I (France)* **3**, 2151 (1993).
- [21] S. M. Barnett and P. L. Knight, *J. Opt. Soc. Am. B* **2**, 467 (1985); *Phys. Rev. A* **38**, 1657 (1988).
- [22] H. Umezawa, H. Matsumoto, and M. Tachiki, *Thermo Field Dynamics and Condensed States* (North-Holland, Amsterdam, 1982); H. Umezawa, *Advanced Field Theory : Micro, Macro, and Thermal physics* (Am. Inst. Phys., New York, 1993).
- [23] E. Yablonovitch, *Phys. Rev. Lett.* **62**, 1742 (1989).
- [24] C. Eberlein, *Zero-Point Fluctuations and Quantum Radiation by Moving Mirrors*, D. Phil. thesis (University of Sussex, 1993).
- [25] I. S. Gradshteyn and I. M. Ryshik, *Tables of Integrals, Series, and Products* (Academic, New York, 1980).
- [26] M. Abramowitz and I. A. Stegun (eds.), *Handbook of Mathematical Functions* (US Govt Printing Office, Washington DC, 1964).
- [27] W. Pauli, *Die allgemeinen Prinzipien der Wellenmechanik*, in “Handbuch der Physik”, vol. V.1, ed. S. Flügge (Springer, Berlin, 1958), section 11.
- [28] L. I. Schiff, *Quantum Mechanics*, 3rd ed. (McGraw-Hill, Singapore, 1968), eq. (35.26).
- [29] Note especially that for $|m\rangle = |k, k'; R\rangle$ the second term on the left-hand side of (3.8) is of order β^2 and can therefore be neglected. Otherwise it would be awkward to deal with, since the argument normally used for non-degenerate states, that $\langle m | (\partial/\partial R) | m \rangle$ is purely imaginary and can thus be absorbed into a physically non-significant phase, does not apply in this case.
- [30] P. A. Maia Neto, *J. Phys. A: Math. Gen.* **27**, 2167 (1994).
- [31] C. Eberlein (work in progress).
- [32] R. Hiller, K. Weninger, S. J. Putterman, and B. P. Barber, *Science* **266**, 248 (1994).
- [33] C. Eberlein, *J. Phys. A: Math. Gen.* **25** 3015 (1992); **25** 3039 (1992).
- [34] The author is indebted to Ken S. Suslick for pointing this out.

Figure captions

Figure 1

The model profile of eq. (4.9) for the squared radius at the collapse of the bubble, printed for four different values of the parameter γ . The solid line corresponds to the function with the largest γ .

Figure 2

The spectral density calculated numerically from eq. (4.5) as a function of photon frequency, for the model profile (4.9) with $R_0 = 45\mu\text{m}$, $R_{\min} = 3\mu\text{m}$, and $\gamma = 10\text{fs}$.

Figure 3

The same data as in figure 2 but as a function of photon wavelength. Note that one can barely make out the features that are clearly visible in figure 2.

Figure 1

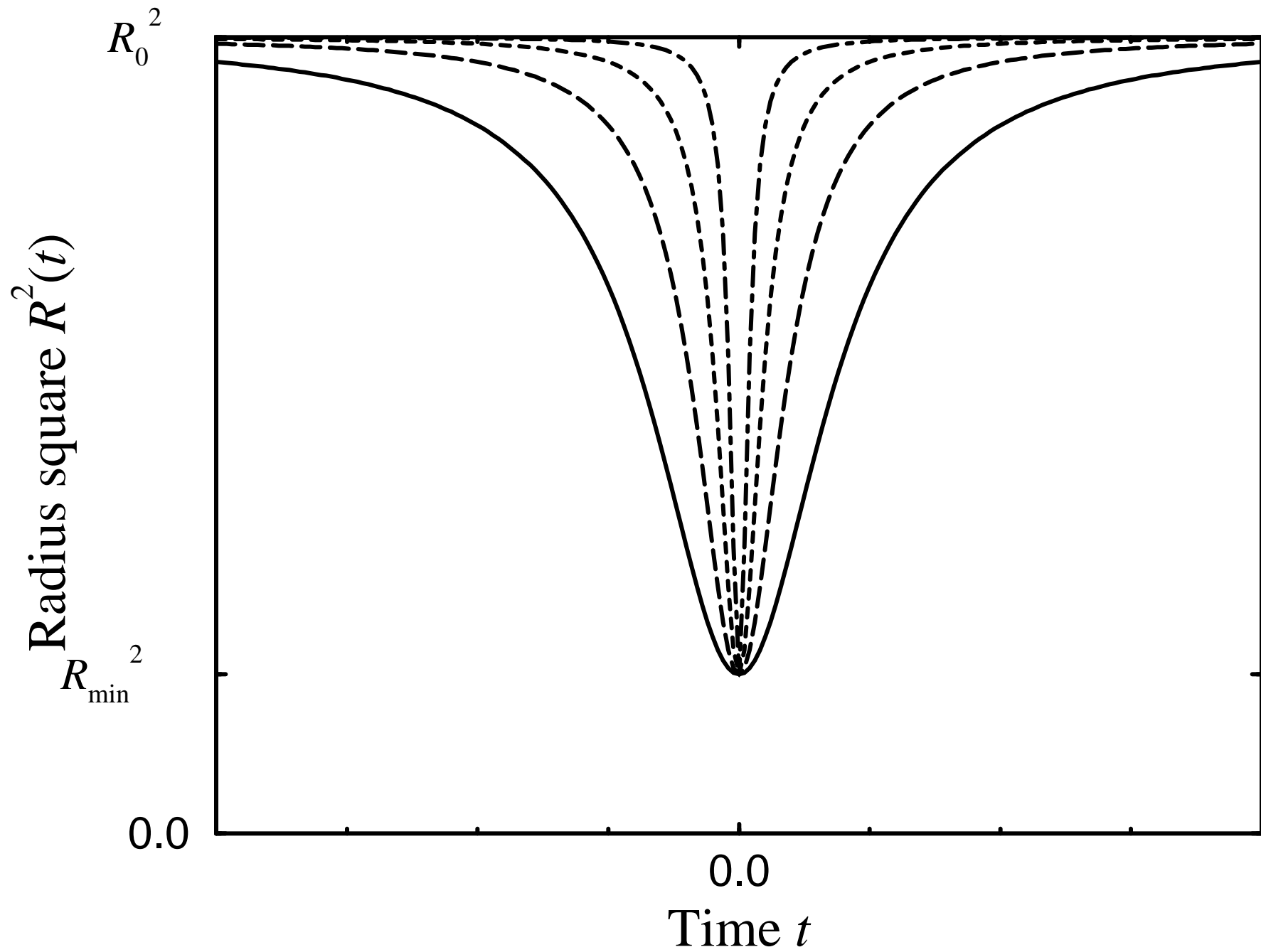


Figure 2

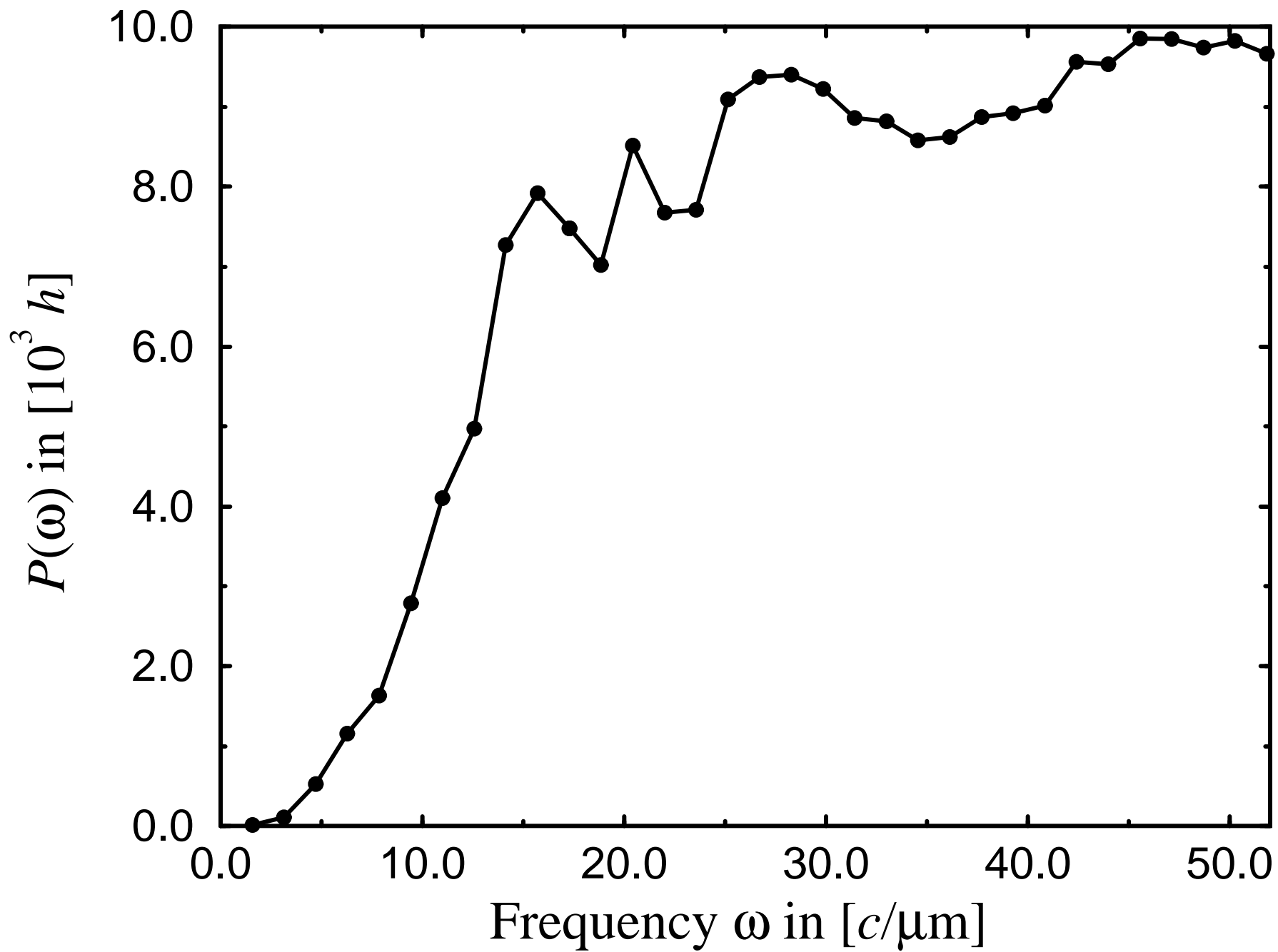


Figure 3

